NASA TECHNICAL NOTE

NASA TN D-4969

C. 1

NASA TN D-4969

A MATHEMATICAL ANALYSIS OF SUPERSONIC INLET DYNAMICS

by Ross G. Willoh

Lewis Research Center
Cleveland, Ohio

NATIONAL AERONAUTICS AND SPACE ADMINISTRATION • WASHINGTON, D. C. • DECEMBER 1968

NASA TN D-4969

A MATHEMATICAL ANALYSIS OF SUPERSONIC INLET DYNAMICS

By Ross G. Willoh

Lewis Research Center
Cleveland, Ohio

NATIONAL AERONAUTICS AND SPACE ADMINISTRATION

For sale by the Clearinghouse for Federal Scientific and Technical Information
Springfield, Virginia 22151 – CFSTI price $3.00

ABSTRACT

An approximate mathematical analysis of supersonic inlet dynamics is presented. The subsonic duct is subdivided into constant-area sections which are represented by one-dimensional wave equations. The movable normal shock is used as the upstream boundary condition, and a choked station is assumed for the downstream boundary condition. The analysis leads to a closed-form matrix solution for the shock-position transfer function. Analytical results are presented and compared with experimental data.

A MATHEMATICAL ANALYSIS OF SUPERSONIC INLET DYNAMICS

by Ross G. Willoh

Lewis Research Center

SUMMARY

An approximate mathematical analysis of supersonic inlet dynamics is presented. The subsonic portion of the inlet is represented by one-dimensional wave equations which are integrable along constant-area portions of the subsonic duct. The complete subsonic duct is thus represented by subdividing it into constant-area sections. The movable normal shock is used as the upstream boundary condition, and a choked station is assumed for the downstream boundary condition. The analysis leads to closed-form matrix solutions for shock position and pressure frequency response. Results from the analysis are presented and compared with test data from an experimental inlet.

INTRODUCTION

Conventional propulsion systems for supersonic aircraft consist of either a turbojet or turbofan engine and a supersonic inlet. The inlet is intended to decelerate the supersonic air stream to velocities suitable for the engine and, in so doing, convert a portion of the free-stream kinetic energy to static pressure. In a mixed-compression inlet, supersonic deceleration is accomplished in a converging section of the inlet duct and subsonic deceleration in a diverging section. The two regimes are separated by a normal shock just downstream of the minimum-area portion of the duct.

Inlet pressure recovery is highest when the normal shock is positioned at, or just downstream of, the minimum-area point. If, however, the shock wave moves upstream of the minimum-area position, it generally becomes unstable and continues to move until it stands in front of the inlet. When the shock is in front of the inlet, engine weight flow and thrust are sharply reduced, and vehicle drag is increased.

Inlets with variable geometry are used to achieve high performance for aircraft operating over a range of supersonic speeds. The use of variable inlet geometry does not in itself guarantee the desired performance, since variable geometry is an asset only when it is properly positioned. Control systems are needed to vary the inlet geometry not only for steady-state flight requirements, but also to minimize the effects of system disturbances arising from gusts, aircraft maneuvers, and changes in engine operation. The design of a high-performance, shock-position-control system requires frequency response data or a mathematical description of shock-position dynamics. The purpose of this report is to develop an approximate mathematical analysis for the dynamics of supersonic inlets. A means for obtaining shock-position frequency response and a mathematical representation suitable for analog simulation are presented.

The theory of shock motion in channel flow is examined in a number of ways in the available literature. One of the earlier reports in the area (ref. 1) is concerned with the stability of shock waves in channel flow. In reference 2, the concept of a Helmholtz resonator is applied to an inlet. In reference 3, the method of coordinate perturbation is applied to the interaction of a disturbance and a shock wave in diffuser flow. In reference 4, a Helmholtz resonator is combined with a single capacitive lump. The analysis of this reference is carried out in detail, and the results are compared with experimental data. In addition, a discussion of the application of the method of characteristics is presented. In reference 5, the effects of pressure disturbances just downstream of the normal shock on shock position are investigated in a linearized analysis.

The experimental investigation of inlet dynamics presented in reference 6 indicates the presence of multiple resonances typical of distributed-parameter systems. Any analysis which predicts such multiple resonances must contain a duct representation which includes distributed effects. The number of lumps needed with conventional lumping techniques rises rapidly with any requirement for accuracy beyond the first resonance. The method presented in this report combines a set of linearized equations across the normal shock with an exact solution of the linearized wave equation. This treatment of the subsonic duct avoids the complexity of the method of characteristics while still predicting the multiple resonances obtained in reference 6. The analysis presented is more exact than conventional lumped-parameter techniques, and for many problems, is no more complicated in application.

MATHEMATICAL ANALYSIS

An idealized one-dimensional inlet is shown schematically in figure 1. The symbols used in this figure and throughout the text are defined in appendix A. A linearized dynamic analysis relating shock position to adjacent parameters is presented in appendix B. Linearized wave equations for the subsonic portion of the duct are developed in appendix C. The shock-position equations become the upstream boundary conditions for the wave equations. A choked exit station was assumed for the downstream boundary condition. The mathematical formulations are based on the selection of flow, total

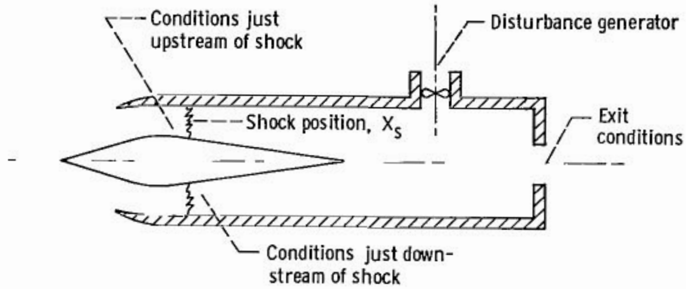

Figure 1. - Idealized mixed-compression inlet.

pressure, and entropy as the independent variables to describe system behavior. Although other parameters may be used, those selected are constant in the steady state, since friction losses are neglected, and thus considerably simplify the linearized analysis.

Shock-Position Dynamics

The equations for shock position are developed in appendix B. Continuity, momentum, and energy balances are taken across the normal shock and modified to account for a moving shock. With the use of the assumptions of perfect-gas relations, a constant specific-heat ratio of 1.4, and negligible change in duct area across the normal shock, the equations are linearized in terms of the selected variables. It is shown in appendix B that

$$\frac{\Delta P_{T,2}}{\overline{P}_{T,2}} = \frac{6}{7\overline{M}_1^2 - 1} \frac{\Delta P_{T,1}}{\overline{P}_{T,1}} - \frac{7\left(\overline{M}_1^2 - 1\right)}{7\overline{M}_1^2 - 1} L_T \frac{A'}{A} \left(\frac{\Delta X_s}{L_T}\right)$$

$$- \frac{7\left(\overline{M}_1^2 - 1\right)}{7\overline{M}_1^2 - 1} L_T \frac{5\left(1 + 0.2\,\overline{M}_1^2\right)^{1/2}}{6\overline{a}_T\overline{M}_1} \frac{d}{dt}\left(\frac{\Delta X_s}{L_T}\right) + \frac{7\left(\overline{M}_1^2 - 1\right)}{7\overline{M}_1^2 - 1}\left(\frac{\Delta \dot{W}_1}{\overline{\dot{W}}} + \frac{\Delta a_{T,1}}{\overline{a}_T}\right) \tag{1}$$

$$\frac{\Delta \dot{W}_2}{\overline{\dot{W}}} = \frac{\Delta \dot{W}_1}{\overline{\dot{W}}} + \frac{1}{\overline{a}_T\overline{M}_1} \frac{\overline{M}_1^2 - 1}{\left(1 + 0.2\,\overline{M}_1^2\right)^{1/2}} L_T \frac{d}{dt}\left(\frac{\Delta X_s}{L_T}\right) \tag{2}$$

$$\frac{\Delta S_2}{R} = \frac{\Delta S_1}{R} - \frac{7\left(\overline{M}_1^2 - 1\right)}{7\overline{M}_1^2 - 1}\left(\frac{\Delta \dot{W}_1}{\overline{\dot{W}}} + \frac{\Delta a_{T,1}}{\overline{a}_T} - \frac{\Delta P_{T,1}}{\overline{P}_T}\right) + \frac{7\left(\overline{M}_1^2 - 1\right)}{7\overline{M}_1^2 - 1} L_T \frac{A'}{A}\left(\frac{\Delta X_s}{L_T}\right)$$

$$- \frac{7\left(\overline{M}_1^2 - 1\right)}{7\overline{M}_1^2 - 1} L_T \frac{\overline{M}_1^2 - 1}{\overline{a}_T \overline{M}_1\left(1 + 0.2\,\overline{M}_1^2\right)^{1/2}} \frac{d}{dt}\left(\frac{\Delta X_s}{L_T}\right) \tag{3}$$

where the subscripts 1 and 2 designate fixed stations just upstream and just downstream of the shock.

The dynamic relations for shock position given in equations (1) to (3) are valid for upstream and downstream perturbations. If only downstream disturbances are considered, $\Delta P_{T,1}$, $\Delta \dot{W}_1$, and ΔS_1 are zero; and equations (1) to (3) can be written in terms of the Laplace transform as

$$\tilde{P}_2 = -C_1\left(L_T \frac{A'}{A} + C_2 s\right)\tilde{X}_s \tag{4}$$

$$\tilde{\dot{W}}_2 = C_3 s \tilde{X}_s \tag{5}$$

$$\tilde{S}_2 = C_1\left(L_T \frac{A'}{A} - C_3 s\right)\tilde{X}_s \tag{6}$$

where

$$C_1 = \frac{7\left(\overline{M}_1^2 - 1\right)}{7\overline{M}_1^2 - 1}$$

$$C_2 = \frac{5\left(1 + 0.2\,\overline{M}_1^2\right)^{1/2}}{6\overline{a}_T \overline{M}_1} L_T$$

$$C_3 = \frac{1}{\overline{a}_T \overline{M}_1} \frac{\overline{M}_1^2 - 1}{\left(1 + 0.2\,\overline{M}_1^2\right)^{1/2}} L_T$$

$$\tilde{P} = \frac{\Delta P_T(s)}{\bar{P}_T}$$

$$\tilde{\dot{W}} = \frac{\Delta \dot{W}(s)}{\bar{\dot{W}}}$$

$$\tilde{X}_s = \frac{\Delta X_s(s)}{L_T}$$

and

$$\tilde{S} = \frac{\Delta S(s)}{R}$$

Subsonic-Duct Equations

The analysis of the subsonic duct is based on a linearization of the compressible-flow equations written in terms of weight flow, total pressure, and entropy. Using the assumptions of perfect-gas relations and an inviscid non-heat-conducting fluid, the following set of equations are developed in appendix C as equations (95):

$$\frac{g}{a\rho_T} \frac{\delta^+ P_T}{\delta t} + \frac{1}{A\rho} \frac{\delta^+ \dot{W}}{\delta t} + \frac{aM(M + 2)}{7R} \frac{\delta^+ S}{\delta t} + \frac{a}{A} \frac{\partial A}{\partial t} = 0$$

$$\frac{g}{a\rho_T} \frac{\delta^- P_T}{\delta t} - \frac{1}{A\rho} \frac{\delta^- \dot{W}}{\delta t} - \frac{aM(2 - M)}{7R} \frac{\delta^- S}{\delta t} + \frac{a}{A} \frac{\partial A}{\partial t} = 0$$

$$\frac{\partial S}{\partial t} + v \frac{\partial S}{\partial x} = 0$$

where

$$\frac{\delta^{\pm}}{\delta t} = \frac{\partial}{\partial t} + (v \pm a) \frac{\partial}{\partial x}$$

After linearization, if area changes are assumed to be slow, these expressions reduce to equations (99) of appendix C.

$$\left[\frac{\partial}{\partial t} + (v + a)\frac{\partial}{\partial x}\right]\left(\frac{\Delta P_T}{\overline{P}_T} + \alpha\frac{\Delta\dot{W}}{\overline{\dot{W}}} + \beta\frac{\Delta S}{R}\right) = 0$$

$$\left[\frac{\partial}{\partial t} + (v - a)\frac{\partial}{\partial x}\right]\left(\frac{\Delta P_T}{\overline{P}_T} - \alpha\frac{\Delta\dot{W}}{\overline{\dot{W}}} - \gamma\frac{\Delta S}{R}\right) = 0$$

$$\left(\frac{\partial}{\partial t} + v\frac{\partial}{\partial x}\right)\left(\frac{\Delta S}{R}\right) = 0$$

where

$$\alpha = \frac{7M_{av}}{M_{av}^2 + 5}$$

$$\beta = \frac{M_{av}(M_{av} + 2)}{M_{av}^2 + 5}$$

$$\gamma = \frac{M_{av}(2 - M_{av})}{M_{av}^2 + 5}$$

The equations of the above set are in the form of wave equations, and their solutions may be written in terms of a time shift. It is thus shown in appendix C that the fluid properties between two stations, 1 and 2, of a subsonic duct can be related in Laplace transform notation by

$$\widetilde{P}_2 + \alpha\widetilde{\dot{W}}_2 + \beta\widetilde{S}_2 = e^{-\sigma s}\left(\widetilde{P}_1 + \alpha\widetilde{\dot{W}}_1 + \beta\widetilde{S}_1\right) \tag{7}$$

$$\widetilde{P}_2 - \alpha\widetilde{\dot{W}}_2 - \gamma\widetilde{S}_2 = e^{\tau s}\left(\widetilde{P}_1 - \alpha\widetilde{\dot{W}}_1 - \gamma\widetilde{S}_1\right) \tag{8}$$

$$\widetilde{S}_2 = e^{-\theta s}\left(\widetilde{S}_1\right) \tag{9}$$

where $\sigma = L/(v + a)$, $\tau = L/(a - v)$, and $\theta = L/v$. The integration over the coordinate x, used in arriving at equations (7) to (9) is based on a constant-area duct. These equations must thus be regarded as a solution for the case of a constant-area duct.

Equation (7) represents the propagation of a wave composed of a linear combination of total pressure, weight flow, and entropy. The wave travels downstream from station 1 to station 2 at a velocity equal to the sum of the fluid velocity and the speed of sound. Equation (8) represents the propagation of a wave composed of another linear combination of the same variables. This wave travels upstream from the second station to the first at a velocity equal to the speed of sound less the flow velocity. Equation (9) represents an entropy wave traveling with the fluid at the fluid velocity.

Since the integration necessary to obtain equations (7) to (9) is valid only for a constant-area duct, variations in duct area are included in the analysis by dividing the duct into sections. The Mach number in each section is averaged by summing one-half of the initial and final values along the section. The parameters α, β, and γ are then computed from the averaged Mach number. The computation of the corresponding delay times σ, τ, and θ is also based on average properties in the section. With the evaluation of these constants, equations (7) to (9) form a set which describes each subsonic section.

Equations (4) to (9) account for shock and subsonic-duct dynamics. The set thus provides a basic mathematical model which can be applied to a supersonic inlet. For the solution of a specific problem, however, the disturbance must be described in terms of the dependent variables, and an equation for the termination of the final subsonic section must be provided.

Disturbance Equations

Although the basic mathematical formulation presented will accommodate various disturbances, consideration will be restricted to flow perturbations introduced in the subsonic duct. Figure 2 illustrates such a disturbance and the notation associated with

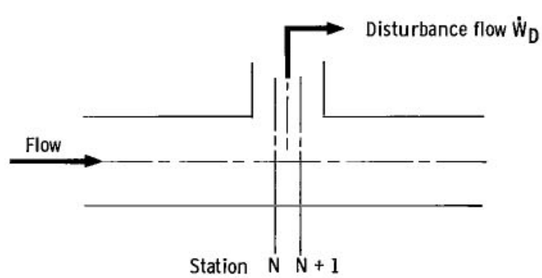

Figure 2. - Flow disturbance in subsonic duct.

it. If the section preceding the disturbance is terminated at station n just before the disturbance, the following equations relating fluid conditions before the disturbance to those just downstream can be written in Laplace transform notation as

$$\tilde{P}_n = \tilde{P}_{n+1} \tag{10}$$

$$\tilde{\dot{W}}_n = \tilde{\dot{W}}_{n+1} + \tilde{\dot{W}}_D \tag{11}$$

$$\tilde{S}_n = \tilde{S}_{n+1} \tag{12}$$

Exit Boundary Condition

The equations applied at the end of the last section depend on the problem boundary conditions. If it is assumed that the inlet is terminated with a choked orifice, the flow can be described by

$$\dot{W}_E = A_E \sqrt{\frac{k}{R}} \frac{P_{T,E}}{\sqrt{\Theta_{T,E}}} \frac{M}{\left(1 + 0.2\ M^2\right)^3} \tag{13}$$

where $M = 1.0$ for a choked orifice, and it is assumed that $k = 1.4$. Linearizing equation (13) and simplifying with

$$\Theta_T\ dS = C_p\ d\Theta_T - \frac{dP_T}{\rho_T}$$

results in

$$\frac{\Delta\dot{W}_E}{\overline{\dot{W}}} = \frac{\Delta A_E}{\overline{A}_E} + \frac{6}{7} \frac{\Delta P_{T,E}}{\overline{P}_T} - \frac{1}{7} \frac{\Delta S_E}{R}$$

or for $\Delta A = 0$, the Laplace transform can be written as

$$\tilde{\dot{W}}_E = \frac{6}{7} \tilde{P}_E - \frac{1}{7} \tilde{S}_E \tag{14}$$

Equation Summary

The shock-position or upstream boundary equations (4) to (6), the subsonic duct equations (7) to (9), the disturbance equations (10) to (12), and the exit boundary condition, equation (14), form a complete set describing shock position to perturbations in duct flow. Rewriting equation (8) as

$$\tilde{P}_1 - \alpha\tilde{W}_1 - \gamma\tilde{S}_1 = e^{-\tau s}\left(\tilde{P}_2 - \alpha\tilde{W}_2 - \gamma\tilde{S}_2\right) \tag{15}$$

allows the direct simulation of the set of equations. In this form, the equations may be represented on a digital computer with one of the simulation languages such as MIMIC (ref. 7)

MATRIX SOLUTION OF EQUATIONS

Mathematical Formulation

Even though direct simulation of the complete set of equations is difficult because of the algebraic complexity, a closed-form matrix solution for the shock-position transfer function can be obtained. This solution can be programmed for the numerical evaluation of the desired transfer function.

In matrix form, the shock-position expressions, equations (4) to (6), become

$$\begin{bmatrix} \tilde{P}_2 \\ \tilde{W}_2 \\ \tilde{S}_2 \end{bmatrix} = \begin{bmatrix} G_{1,1} & 0 & 0 \\ G_{2,1} & 0 & 0 \\ G_{3,1} & 0 & 0 \end{bmatrix} \begin{bmatrix} \tilde{X}_s \\ 0 \\ 0 \end{bmatrix} \tag{16}$$

or

$$T_2 = GX \tag{17}$$

If station 2, just downstream of the shock, is separated from station 3 by a section of subsonic duct, equations (7) to (9) can be used to relate conditions at the two stations. In matrix notation these equations become

$$\begin{bmatrix} 1 & \alpha_1 & \beta_1 \\ 1 & -\alpha_1 & -\gamma_1 \\ 0 & 0 & 1 \end{bmatrix} \begin{bmatrix} \tilde{P}_3 \\ \tilde{\dot{W}}_3 \\ \tilde{S}_3 \end{bmatrix} = \begin{bmatrix} e^{-\sigma_1 s} & 0 & 0 \\ 0 & e^{\tau_1 s} & 0 \\ 0 & 0 & e^{-\theta_1 s} \end{bmatrix} \begin{bmatrix} 1 & \alpha_1 & \beta_1 \\ 1 & -\alpha_1 & -\gamma_1 \\ 0 & 0 & 1 \end{bmatrix} \begin{bmatrix} \tilde{P}_2 \\ \tilde{\dot{W}}_2 \\ \tilde{S}_2 \end{bmatrix} \tag{18}$$

or

$$B_2 T_3 = D_2 B_2 T_2 \tag{19}$$

In a similar manner, stations k and $k+1$ are related by

$$B_k T_{k+1} = D_k B_k T_k \tag{20}$$

In matrix form the expressions describing the disturbance flow, equations (10) to (12), become

$$\begin{bmatrix} \tilde{P}_{n+1} \\ \tilde{\dot{W}}_{n+1} \\ \tilde{S}_{n+1} \end{bmatrix} = \begin{bmatrix} \tilde{P}_n \\ \tilde{\dot{W}}_n \\ \tilde{S}_n \end{bmatrix} - \begin{bmatrix} 0 \\ \tilde{\dot{W}}_D \\ 0 \end{bmatrix} \tag{21}$$

or

$$T_{n+1} = T_n - T_D \tag{22}$$

while equation (14) for the exit boundary condition becomes

$$\begin{bmatrix} 1 & -7/6 & -1/6 \\ 0 & 0 & 0 \\ 0 & 0 & 0 \end{bmatrix} \begin{bmatrix} \tilde{P}_j \\ \tilde{\dot{W}}_j \\ \tilde{S}_j \end{bmatrix} = 0 \tag{23}$$

or

$$FT_j = 0 \tag{24}$$

Equations (17), (19), (20), (22), and (24) can be combined to represent the inlet dynamics.

$$\left.\begin{aligned}
T_2 &= GX \\
B_2T_3 &= D_2B_2T_2 \\
B_3T_4 &= D_3B_3T_3 \\
&\;\;\vdots \\
B_{n-1}T_n &= D_{n-1}B_{n-1}T_{n-1} \\
T_{n+1} &= T_n - T_D \\
B_{n+1}T_{n+2} &= D_{n+1}B_{n+1}T_{n+1} \\
&\;\;\vdots \\
B_{j-1}T_j &= D_{j-1}B_{j-1}T_{j-1} \\
FT_j &= 0
\end{aligned}\right\} \qquad (25)$$

Defining $E_k = B_k^{-1}D_kB_k$ (where B^{-1} is the inverse of the B matrix) allows considerable simplification of equations (25). The B^{-1} and E matrices are

$$B^{-1} = \begin{bmatrix} \frac{1}{2} & \frac{1}{2} & \frac{\gamma - \beta}{2} \\ \frac{1}{2\alpha} & -\frac{1}{2\alpha} & -\frac{\gamma + \beta}{2\alpha} \\ 0 & 0 & 1 \end{bmatrix}$$

The E matrix can be defined by its elements $\epsilon_{i,j}$

$$\epsilon_{1,1} = \frac{e^{-\sigma s} + e^{\tau s}}{2}$$

$$\epsilon_{1,2} = \frac{\alpha(e^{-\sigma s} - e^{\tau s})}{2}$$

$$\epsilon_{1,3} = \frac{\beta(e^{-\sigma s} - e^{-\theta s})}{2} - \frac{\gamma(e^{\tau s} - e^{-\theta s})}{2}$$

$$\epsilon_{2,1} = \frac{\epsilon_{1,2}}{\alpha^2}$$

$$\epsilon_{2,2} = \epsilon_{1,1}$$

$$\epsilon_{2,3} = \frac{\beta(e^{-\sigma s} - e^{-\theta s})}{2\alpha} + \frac{\gamma(e^{\tau s} - e^{-\theta s})}{2\alpha}$$

$$\epsilon_{3,1} = 0$$

$$\epsilon_{3,2} = 0$$

$$\epsilon_{3,3} = e^{-\theta s}$$

With these definitions, equations (25) can be written as

$$\left.\begin{aligned} T_n &= E_{n-1}E_{n-2} \cdot \cdot \cdot E_3E_2GX \\ T_{n+1} &= T_n - T_D \\ T_j &= E_{j-1}E_{j-2} \cdot \cdot \cdot E_{n+2}E_{n+1}T_{n+1} \\ FT_j &= 0 \end{aligned}\right\} \qquad (26)$$

If the products of E matrices are replaced by

$$K = E_{n-1}E_{n-2} \cdot \cdot \cdot E_3E_2$$

and

$$N = E_{j-1}E_{j-2} \cdot \cdot \cdot E_{n+2}E_{n+1}$$

equations (26) become

$$\left.\begin{aligned} T_n &= KGX \\ T_{n+1} &= T_n - T_D \\ T_j &= NT_{n+1} \\ FT_j &= 0 \end{aligned}\right\} \tag{27}$$

Equations (27) can be combined into

$$FNKGX = FNT_D \tag{28}$$

Since FNKG has only a single nonzero element because F is a single-row matrix and G is a single-column matrix, equation (28) can be written as

$$F_{1,\alpha}N_{\alpha,\beta}K_{\beta,\gamma}G_{\gamma,1}X_1 = F_{1,\alpha}N_{\alpha,2}T_{D,2} \tag{29}$$

where the summation convention (summation across repeated subscripts) is assumed. As $X_1 = \tilde{X}_s$ and $T_{D,2} = \tilde{\dot{W}}_D$, then

$$\frac{\tilde{X}_s}{\tilde{\dot{W}}_D} = \frac{F_{1,\alpha}N_{\alpha,2}}{F_{1,\alpha}N_{\alpha,\beta}K_{\beta,\gamma}G_{\gamma,1}} \tag{30}$$

The elements of the N, K, and G matrices are functions of s. Equation (30) thus represents the transfer function for the response of shock position to the flow disturbance assumed. For $s = i\omega$, the frequency response, in amplitude and phase, is easily and quickly calculated numerically by making the operations indicated by equation (30) in complex algebra. Substituting these results for shock-position response into the first of equations (25) gives the response for the elements of T_2; substituting these results into the second of equations (25) gives the response for the elements of T_3, etc. Thus, the frequency response for perturbations in total pressure, flow rate, and entropy are obtained at all stations.

The perturbations in other inlet variables, such as static pressure, velocity, etc., can be obtained at each station from those in total pressure, flow rate, and entropy. An example of this is given later (eq. (34)).

Comparison of Analysis with Test Data

Frequency response tests were conducted on a 48-centimeter mixed-compression inlet in the Lewis Research Center 10- by 10-foot supersonic wind tunnel. A detailed description of the inlet is reported in reference 8, and the data resulting from the frequency response test program and a description of the disturbance device are reported in reference 6. To verify the analytical approach presented in this report, the techniques have been applied to this 48-centimeter inlet.

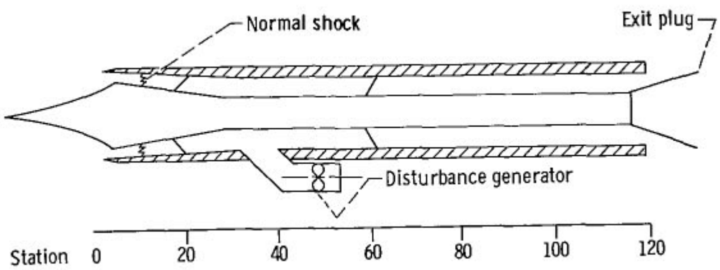

Figure 3. - Mixed-compression, 48-centimeter inlet.

A schematic diagram of the 48-centimeter mixed-compression inlet is presented in figure 3. The variable-area portion of the inlet, beginning at the shock and extending to the disturbance generator, was divided into three sections of equal length. The remainder of the inlet, extending from the disturbance generator to the choked exit, was represented by a single section. With this sectioning, equations (26) become

$$\left.\begin{aligned} T_5 &= E_4E_3E_2GX \\ T_6 &= T_5 - T_D \\ T_7 &= E_6T_6 \\ FT_7 &= 0 \end{aligned}\right\} \quad (31)$$

or, after appropriate manipulation,

$$FE_6E_4E_3E_2GX = FE_6T_D \tag{32}$$

A schematic diagram of the inlet is presented in figure 4 to indicate the sectioning techniques and the location of significant problem variables. Table I contains numerical values associated with the tests of the 48-centimeter inlet. In addition, coefficients, based on steady-state, one-dimensional flow calculations averaged across each section, are presented for use in the evaluation of equations (31) and (32).

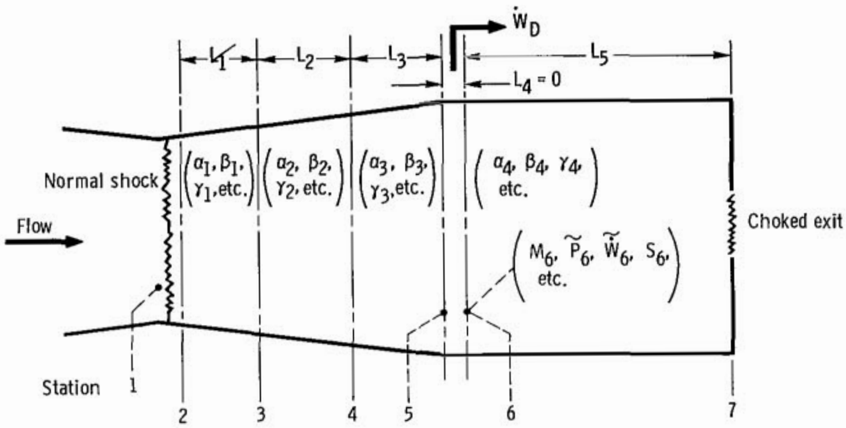

Figure 4. - Schematic indicating station numbers and associated parameter subscripts.

TABLE I. - NUMERICAL VALUES FOR 48-CENTIMETER-INLET

COEFFICIENTS BETWEEN STATIONS

[Coefficients for shock conditions: $C_1 = 0.3133$; $C_2 = 5.483\times10^{-3}$ sec; $C_3 = 2.013\times10^{-3}$ sec. Test conditions: total pressure, 2534.4 lb/ft^2 (121 130 N/m^2); total temperature, 689.3° R (382.9 K); area ratio A'/A, 0.4165 ft^{-1} (1.366 m^{-1}).]

Station	Coefficient			Transportation time, sec		
	α	β	γ	σ	θ	τ
2 to 3	0.9225	0.3597	0.1675	0.2961×10^{-3}	0.7034×10^{-3}	1.872×10^{-3}
3 to 4	.6752	.2418	.1440	.3309	.9845	1.009
4 to 5	.4956	.1673	.1159	.4573	1.716	.9789
6 to 7	.4222	.1392	.1021	4.075	17.44	7.690

A digital program to perform the necessary operations was written in FORTRAN IV. The coefficients required for the various matrices are placed in storage and subsequently used to calculate the matrix elements. The matrices are formed as arrays from these elements, and the matrix multiplications of equation (32) are then performed. Both the G matrix and the E matrices contain the Laplace transform operator s which is replaced by $i\omega$ for numerical evaluation of the frequency response. These matrices and their products contain complex numbers, and the program is thus written in complex algebra.

The general scheme is to select a frequency value ω and compute the amplitude and phase of the complex number

$$\frac{\tilde{X}_s(i\omega)}{\tilde{\dot{W}}_D(i\omega)} = H(i\omega) = b_3 + id_3 \tag{33}$$

which results from the evaluation of equation (32). The frequency value is then incremented, and the procedure is repeated. The resulting tabulation yields data for a plot of the shock-position-to-disturbance-flow frequency response.

After evaluation, the shock-position-to-disturbance-flow transfer function was used with equations (31) to evaluate the response of the pressure immediately downstream of the shock. Equations (31), however, are written in terms of total pressure, while available test data is in static pressure. The equation relating static pressure to the system dependent variables at some station j is

$$\left(\frac{\Delta P_s}{\overline{P}_s}\right)_j = \left[\frac{\overline{M}^2 + 5}{5\left(1 - \overline{M}^2\right)} \frac{\Delta P_T}{\overline{P}_T} - \frac{7\overline{M}^2}{5\left(1 - \overline{M}^2\right)} \frac{\Delta \dot{W}}{\overline{\dot{W}}} - \frac{\overline{M}^2}{5\left(1 - \overline{M}^2\right)} \frac{\Delta S}{R}\right]_j \tag{34}$$

Equation (34) was used with equations (31) in the actual evaluation of the static-pressure responses presented.

Figures 5 and 6 contain the results of the computations plotted with the corresponding test data from reference 6. The amplitude ratios are plotted in normalized form; that is, the amplitude ratio measured at the test frequency is divided by the amplitude ratio determined at a low reference frequency.

Figure 5 contains the shock-position-to-disturbance-flow data. The figure indicates the good agreement that was achieved between the experimental and analytical shock-position results.

Figure 6 contains response plots for static pressure just past the normal shock to disturbance flow. Again, both test data and analytical results are presented. Although

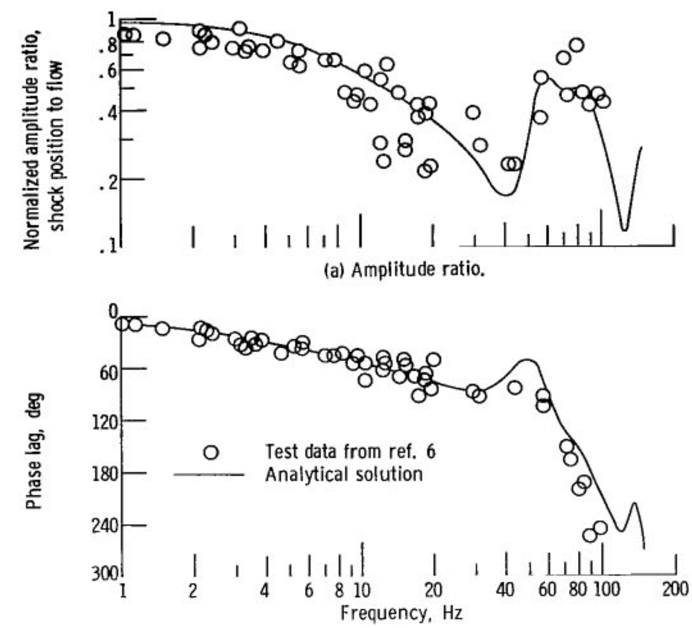

(b) Phase angle.

Figure 5. - Shock-position response to flow perturbations.

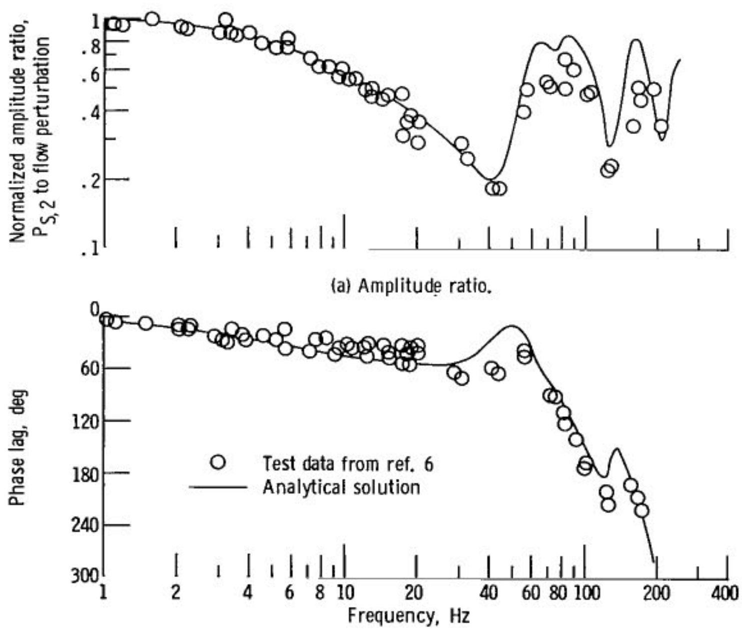

(b) Phase angle.

Figure 6. - Response of static pressure just downstream of shock to flow perturbations.

the test results have slightly less peaking than predicted by the analysis, agreement is reasonably good.

Model Simplification

As previously indicated, the complexity of the waves arriving at the nodes between the sections of the subsonic duct complicates the simulation of the system equations. An examination of the subsonic-duct equations (7) to (9) reveals that the model complexity would be greatly reduced if constant entropy were assumed. Although such an assumption is in no way required for the evaluation of inlet transfer functions through numerical calculations, it is required for any reasonably simple simulation of the inlet.

If constant entropy is assumed, a change in the zero-frequency shock-position gain results. This gain change arises from the system boundary-condition equations. Applying the final-value theorem to equations (4) and (6) allows evaluation of the steady-state-pressure-to-shock-position and entropy-to-shock-position zero-frequency gains.

$$\left.\frac{\tilde{P}_2}{\tilde{X}_s}\right|_{\omega\to 0} = -C_1 L_T \frac{A'}{A}$$

$$\left.\frac{\tilde{S}_2}{\tilde{X}_s}\right|_{\omega\to 0} = C_1 L_T \frac{A'}{A}$$

The exit boundary condition is given in equation (14) as

$$\tilde{\dot{W}}_E = \frac{6}{7}\tilde{P}_E - \frac{1}{7}\tilde{S}_E$$

This equation, together with the zero-frequency gains at the inlet boundary, implies that

$$\left.\frac{\tilde{P}_E}{\tilde{\dot{W}}_E}\right|_{\omega\to 0} = 1$$

If, however, $\tilde{S}$ is set equal to zero throughout the problem, equation (14) becomes

$$\tilde{\dot{W}}_E = \frac{6}{7}\tilde{P}_E$$

which implies that

$$\left.\frac{\widetilde{P}_E}{\widetilde{\dot{W}}_E}\right|_{\omega \to 0} = \frac{7}{6}$$

Thus, the assumption of $\Delta S = 0$ results in a system gain change. To avoid this change, the simplified model assumed that equation (14) could be modified to

$$\widetilde{\dot{W}}_E = \widetilde{P}_E$$

which is equivalent to assuming constant temperature at the exit boundary and constant entropy elsewhere in the system.

To evaluate the effects of the model simplification, the frequency response of the four-section model was numerically evaluated with and without the simplifications. Figure 7 contains plots of the numerical data. Examination of the curves plotted in figure 7

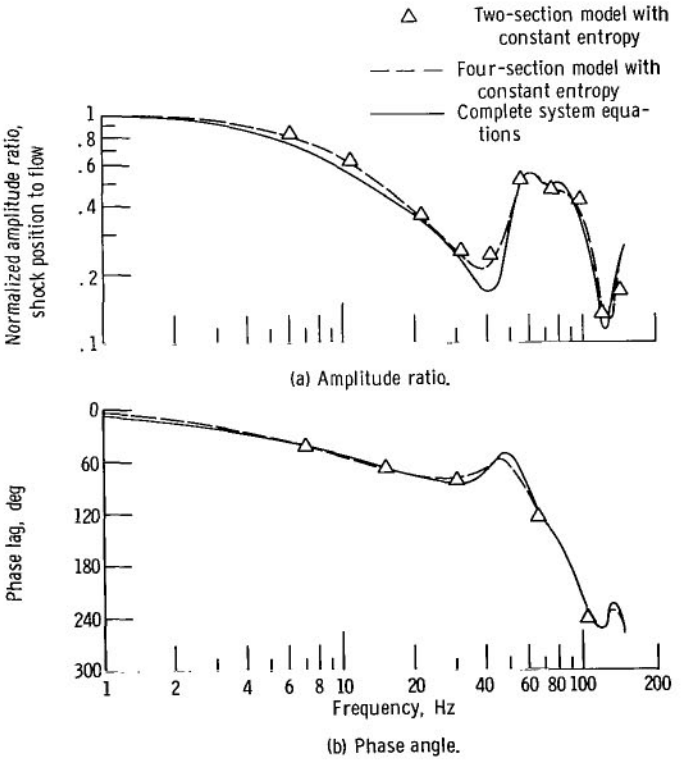

Figure 7. - Shock-position response to flow perturbations. Computed from mathematical model with and without simplications.

indicates that for the inlet considered herein, the simplified model yields good agreement in the frequency range of interest.

To investigate the possibility of further simplification, the frequency response of the simplified system was evaluated with a two-section representation where the variable-area portion of the duct was represented by a single section. The results of these calculations are also plotted in figure 7. The additional simplification did not significantly alter the results.

Analog Simulation

The matrix methods presented yield frequency response data for the inlet dynamics. To secure results in the time domain and to provide a working model for control-system synthesis, an analog simulation was investigated. Since the numerical evaluation of the system equations indicated that a two-section, constant-entropy representation gives reasonable agreement with the test data, this representation was made the basis for an analog simulation. The system transportation times (σ and τ) were represented with the fourth-order Padé approximations of reference 9. Frequency response data obtained

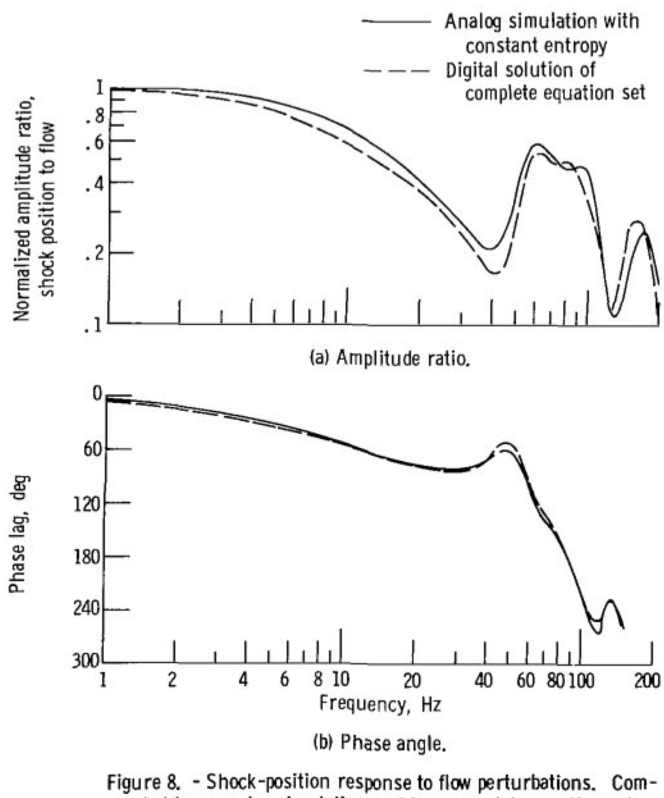

Figure 8. - Shock-position response to flow perturbations. Computed from analog simulation and from complete equation set.

from the analog simulation are plotted in figure 8 along with the digital solution for the complete set of equations. The agreement shown in this figure is excellent to frequencies as high as 200 hertz. The growing discrepancies beyond 200 hertz can be attributed to the Padé approximations whose accuracy deteriorates with rising frequency.

Figure 9 contains a shock-position, time-history response to a step change in bleed flow, obtained from an analog simulation with Padé approximations used for the delay-time representation. Once established, the analog simulation can be used as a design tool for inlet shock-position-control design and experimentation.

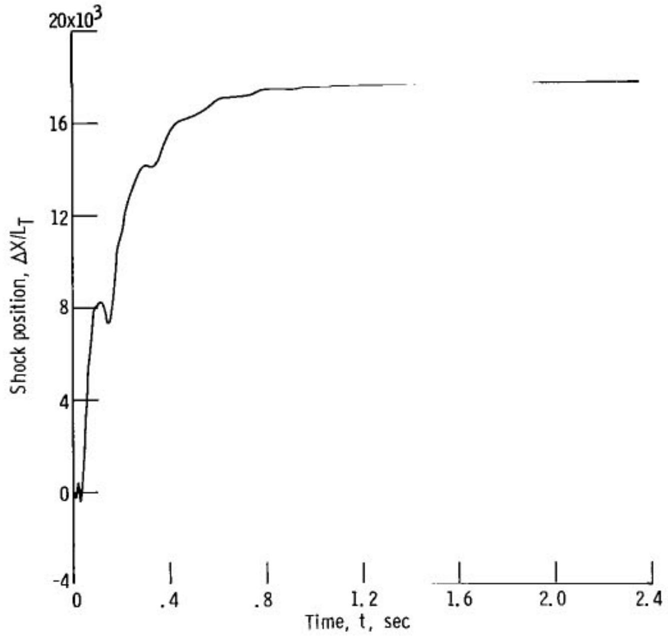

Figure 9. - Shock-position response to step change in bleed flow, analog computer simulation.

CONCLUDING REMARKS

A theory for supersonic inlet dynamics has been presented based primarily on the closed-form solution of the linearized one-dimensional distributed-parameter wave equations. For transfer functions, closed-form expressions were obtained in terms of matrix operations (no matrix inversion required). For numerical evaluation of frequency responses, these matrix operations can be simply programmed on a digital computer in complex algebra. The results of the theory were found to be in excellent agreement with data from a 48-centimeter inlet. Various further simplifications to the theory were evaluated. The theory developed herein can be applied also to analog computer simulation.

In the application of the methods presented to the prediction of shock-position dynamics, difficulty arises in the selection of an appropriate value of A'/A (i. e., $(1/A)(dA/dx)$ in the vicinity of the normal shock) to be used. Because of boundary layer effects and flow distortion in the throat region, shock dynamics are not uniquely dependent on the geometric A'/A. The value used in the analysis should thus include the influence of the boundary layer as well as the inlet geometry. Further work is required to allow the analytical determination of an effective A'/A parameter.

In general, results obtained from both the full and simplified models compare well with test data obtained from experimental inlets. Further work must be done to determine the regions to which the model can be successfully applied, and to include the effects of performance bleed and other variations on the basic inlet.

Lewis Research Center,
National Aeronautics and Space Administration,
Cleveland, Ohio, August 28, 1968,
720-03-01-04-22.

APPENDIX A

SYMBOLS

A	cross-sectional area, ft^2; m^2
A'	rate of change of cross-sectional area along duct, ft^2/ft; m^2/m
a	speed of sound, ft/sec; m/sec
B	coefficient matrix
b_n	constant coefficients (n = integer), appropriate dimensions
C_p	specific heat at constant pressure, ft-lb/(lb)(^oR); m/K
C_v	specific heat at constant volume, ft-lb/(lb)(^oR); m/K
C_1	coefficient, nondimensional
C_2	coefficient, sec
C_3	coefficient, sec
D	delay matrix
d_n	constant coefficients (n = integer), appropriate dimensions
E	coefficient matrix
$\mathcal{E}$	functional parameter defined in eqs. (100)
F	coefficient matrix
G	shock-position transfer function matrix
g	gravitational constant, unit force/unit mass
H	general functional relation
h	enthalpy, ft-lb/lb; m
i	$\sqrt{-1}$
K	matrix
k	ratio of specific heats
L	length, ft; m
L_T	duct length from normal shock to exit station, ft; m
M	Mach number
$M_{1,R}$	relative Mach number at station 1
N	coefficient matrix
P	pressure, lb/ft^2; N/m^2
Q	heat, ft-lb/lb; m
R	universal gas constant, ft/^oR; m/K
S	entropy, ft-lb/(lb)(^oR); m/K
s	Laplace transform operator
T	column matrix
t	time, sec
v	velocity, ft/sec; m/sec
$\dot{W}$	weight flow, lb/sec; kg/sec
X	shock-position column matrix
X_s	shock-position, ft; m
x	space coordinate, ft; m
α	coefficient, nondimensional
β	coefficient, nondimensional
γ	coefficient, nondimensional
Δ	perturbation quantity
ϵ	elements of E matrix

η	functional parameter defined in eqs. (100)
Θ	absolute temperature, $^{\circ}$R; K
θ	transportation time, defined in eqs. (105), sec
ξ	functional parameter defined in eqs. (100)
ρ	weight density, lb/ft^3; kg/m^3
σ	transportation time, defined in eqs. (105), sec
τ	transportation time, defined in eqs. (105), sec
ω	frequency, radian/sec

Subscripts:

av	steady-state value of Mach number averaged over section of subsonic duct
D	disturbance variable
E	exit conditions
j, k, n	station number associated with variable
r	reference state
s	static condition
T	total or stagnation condition
α, β, γ	matrix subscript indicating variable location in matrix array
1, 2, 3, . . .	station number associated with variable, or variable location in matrix array

Superscripts:

$(\bar{\ })$	steady-state value of variable
$(\tilde{\ })$	Laplace transform of nondimensional small perturbation variable
$(\dot{\ })$	first derivative of variable with respect to time

APPENDIX B

SHOCK-POSITION EQUATIONS

For a stationary normal shock in a steady flow field, the continuity equation across the shock may be written as

$$\rho_1 A_1 v_1 = \rho_2 A_2 v_2 \tag{35}$$

where stations 1 and 2 are fixed stations just upstream and just downstream of the normal shock as shown in sketch a.

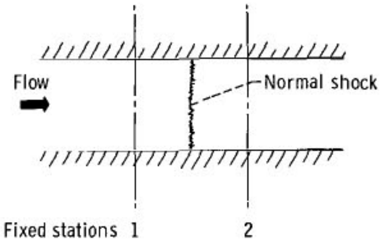

(a)

Since shock thickness is quite small, static relations across a stationary shock may be applied to a moving normal shock if instantaneous velocities are measured relative to the shock and stations 1 and 2 are assumed to be a fixed distance from the shock and, hence, moving with the shock. Under these conditions equation (35) becomes

$$\rho_1 A_1 (v_1 - \dot{X}_s) = \rho_2 A_2 (v_2 - \dot{X}_s) \tag{36}$$

When the analysis is restricted to small perturbations in shock position X_s, and with $A_1 \cong A_2$, equation (36) becomes

$$\dot{W}_2 = \dot{W}_1 + \rho_1 \left(\frac{\rho_2}{\rho_1} - 1 \right) A_1 \dot{X}_s \tag{37}$$

The density relation across the moving normal shock is

$$\frac{\rho_2}{\rho_1} = \frac{6M_{1,R}^2}{M_{1,R}^2 + 5} \tag{38}$$

where $M_{1,R}$, the relative Mach number, is defined by

$$M_{1,R} = M_1 - \frac{\dot{X}_s}{a_1} \tag{39}$$

Combining equations (37) and (38) gives

$$\dot{W}_2 = \dot{W}_1 + \rho_1 A_1 \frac{5\left(M_{1,R}^2 - 1\right)}{M_{1,R}^2 + 5} \dot{X}_s \tag{40}$$

or

$$\dot{W}_2 = \dot{W}_1 \left[1 + \frac{5}{a_{T,1}} \frac{\left(1 + 0.2\ M_1^2\right)^{1/2}}{M_1} \frac{\left(M_{1,R}^2 - 1\right)}{M_{1,R}^2 + 5} \dot{X}_s\right] \tag{41}$$

Linearizing equation (41) and noting that in the steady state $\dot{X}_s$ is zero and $\overline{M}_{1,R} = \overline{M}_1$ (where a bar over a quantity designates the steady-state value of the quantity) result in

$$\frac{\Delta\dot{W}_2}{\overline{\dot{W}}} = \frac{\Delta\dot{W}_1}{\overline{\dot{W}}} + \frac{1}{\overline{a}_T\overline{M}_1} \frac{\overline{M}_1^2 - 1}{\left(1 + 0.2\ \overline{M}_1^2\right)^{1/2}} \Delta\dot{X}_s \tag{42}$$

When stagnation conditions are defined in terms of zero velocity relative to the duct and the perfect-gas law is applied at stations 1 and 2, it can be shown that

$$P_{T,2} = P_{T,1}\left(\frac{P_2}{P_1}\right)^{-5/2}\left(\frac{\rho_2}{\rho_1}\right)^{7/2}\left(\frac{\Theta_{T,2}}{\Theta_{T,1}}\right)^{7/2} \tag{43}$$

or

$$P_{T,2} = P_{T,1}\left(\frac{7M_{1,R}^2 - 1}{6}\right)^{-5/2}\left(\frac{6M_{1,R}^2}{M_{1,R}^2 + 5}\right)^{7/2}\left(\frac{\Theta_{T,2}}{\Theta_{T,1}}\right)^{7/2} \tag{44}$$

Linearizing equation (44) yields

$$\frac{\Delta P_{T,2}}{\overline{P}_{T,2}} = \frac{\Delta P_{T,1}}{\overline{P}_{T,1}} + 3.5\left(\frac{\Delta\Theta_{T,2}}{\overline{\Theta}_T} - \frac{\Delta\Theta_{T,1}}{\overline{\Theta}_T}\right) - 35\,\frac{\left(\overline{M}_1^2 - 1\right)^2}{\left(7\overline{M}_1^2 - 1\right)\left(\overline{M}_1^2 + 5\right)}\,\frac{\Delta M_{1,R}}{\overline{M}_1} \tag{45}$$

where $\overline{\Theta}_{T,1} = \overline{\Theta}_{T,2} = \overline{\Theta}_T$.

The energy equation across the shock may be written as

$$h_1 + \frac{\left(v_1 - \dot{X}_s\right)^2}{2g} = h_2 + \frac{\left(v_2 - \dot{X}_s\right)^2}{2g} \tag{46}$$

The total enthalpy may be computed from

$$h_T = C_p\Theta_T = h + \frac{v^2}{2g} \tag{47}$$

or

$$\left.\begin{aligned} h_1 &= C_p\Theta_{T,1} - \frac{v_1^2}{2g} \\ h_2 &= C_p\Theta_{T,2} - \frac{v_2^2}{2g} \end{aligned}\right\} \tag{48}$$

Substituting equations (48) into equation (46)

$$\Theta_{T,1} - \Theta_{T,2} = \frac{\dot{X}_s}{gC_p}\left(v_1 - v_2\right) \tag{49}$$

Noting that $(v_1 - v_2) \equiv (v_1 - \dot{X}_s) - (v_2 - \dot{X}_s)$ yields

$$v_1 - v_2 = a_1 M_{1,R} - a_2 M_{2,R} \tag{50}$$

but

$$a_2 M_{2,R} = \frac{a_1\left(M_{1,R}^2 + 5\right)}{6M_{1,R}} \tag{51}$$

therefore,

$$v_1 - v_2 = \frac{5a_1}{6M_{1,R}}\left(M_{1,R}^2 - 1\right) \tag{52}$$

Combining equations (52) and (49) gives

$$\Theta_{T,2} = \Theta_{T,1} - \frac{\dot{X}_s}{gC_p}\,\frac{5a_1}{6M_{1,R}}\left(M_{1,R}^2 - 1\right)$$

or

$$\frac{\Theta_{T,2}}{\Theta_{T,1}} = 1 - \frac{\dot{X}_s}{3M_{1,R}a_{T,1}}\,\frac{M_{1,R}^2 - 1}{\left(1 + 0.2\ M_1^2\right)^{1/2}} \tag{53}$$

Linearizing equation (53) and again noting that $\bar{\dot{X}}_s = 0$ yields

$$\left(\frac{\Delta\Theta_{T,2}}{\bar{\Theta}_T} - \frac{\Delta\Theta_{T,1}}{\bar{\Theta}_T}\right) = -\frac{1}{3\bar{a}_T\bar{M}_1}\left[\frac{\bar{M}_1^2 - 1}{\left(1 + 0.2\ \bar{M}_1^2\right)^{1/2}}\right]\Delta\dot{X}_s \tag{54}$$

The relative Mach number $M_{1,R}$ was defined in equation (39) as

$$M_{1,R} = M_1 - \frac{\dot{X}_s}{a_1}$$

which is equivalent to

$$M_{1,R} = M_1 - \frac{\dot{X}_s}{a_{T,1}} \left(1 + 0.2\, \overline{M}_1^2\right)^{1/2} \tag{55}$$

Linearizing equation (55) yields

$$\Delta M_{1,R} = \Delta M_1 - \frac{\left(1 + 0.2\, \overline{M}_1^2\right)^{1/2}}{\overline{a}_T} \Delta \dot{X}_s \tag{56}$$

At station 1 just upstream of the shock $M_1 = v_1/a_1$ and $v_1 = \dot{W}_1/\rho_1 A_1$. Thus,

$$M_1 = \frac{\dot{W}_1}{\rho_1 A_1 a_1} \tag{57}$$

Combining equation (57) with the perfect-gas relation and using total pressure yields

$$M_1 - \frac{5 a_{T,1} \dot{W}_1}{7 g P_{T,1} A_1} \left(1 + 0.2\, M_1^2\right)^3 = 0 \tag{58}$$

Linearizing equation (58) yields

$$\Delta M_1 = \frac{\overline{M}_1\left(5 + \overline{M}_1^2\right)}{5\left(\overline{M}_1^2 - 1\right)} \left(\frac{\Delta P_{T,1}}{\overline{P}_{T,1}} + \frac{\Delta A_1}{\overline{A}_1} - \frac{\Delta \dot{W}_1}{\overline{\dot{W}}} - \frac{\Delta a_{T,1}}{\overline{a}_T}\right) \tag{59}$$

Combining equations (45), (54), (56), and (59) results in

$$\frac{\Delta P_{T,2}}{\overline{P}_{T,2}} = \frac{6}{7\overline{M}_1^2 - 1} \frac{\Delta P_{T,1}}{\overline{P}_{T,1}} - \frac{7\left(\overline{M}_1^2 - 1\right)}{7\overline{M}_1^2 - 1} L_T \left[\frac{A'}{A} \frac{\Delta X_s}{L_T} + \frac{5\left(1 + 0.2\, \overline{M}_1^2\right)^{1/2}}{6 \overline{a}_T \overline{M}_1} \frac{\Delta \dot{X}_s}{L_T}\right]$$

$$+ \frac{7\left(\overline{M}_1^2 - 1\right)}{7\overline{M}_1^2 - 1} \left(\frac{\Delta \dot{W}_1}{\overline{\dot{W}}} + \frac{\Delta a_{T,1}}{\overline{a}_T}\right) \tag{60}$$

where A'/A is dA/dx at the steady-state shock location divided by the area A.

The equation

$$\frac{P}{\rho^k} = \frac{P_r}{\rho_r^k} \exp\left(\frac{S - S_r}{C_v}\right) \tag{61}$$

can be written as

$$\left(\frac{P_2}{P_1}\right)^{5/2} \left(\frac{\rho_2}{\rho_1}\right)^{-7/2} = \exp\left(\frac{S_2 - S_1}{R}\right) \tag{62}$$

or

$$\frac{S_2}{R} - \frac{S_1}{R} = \ln\left[\left(\frac{M_{1,R}^2 + 5}{6M_{1,R}^2}\right)^{7/2} \left(\frac{7M_{1,R}^2 - 1}{6}\right)^{5/2}\right] \tag{63}$$

Linearizing equation (63)

$$\frac{\Delta S_2}{R} - \frac{\Delta S_1}{R} = \frac{35\left(\overline{M}_1^2 - 1\right)^2}{\overline{M}_1\left(\overline{M}_1^2 + 5\right)\left(7\overline{M}_1^2 - 1\right)} \Delta M_{1,R} \tag{64}$$

Combining equation (64) with equations (56) and (59) results in

$$\frac{\Delta S_2}{R} = \frac{\Delta S_1}{R} - \frac{7\left(\overline{M}_1^2 - 1\right)}{7\overline{M}_1^2 - 1}\left(\frac{\Delta\dot{W}_1}{\overline{\dot{W}}} + \frac{\Delta a_{T,1}}{\overline{a}_T}\right) + \frac{7\left(\overline{M}_1^2 - 1\right)}{7\overline{M}_1^2 - 1} \frac{\Delta P_{T,1}}{\overline{P}_{T,1}}$$
$$+ \frac{7\left(\overline{M}_1^2 - 1\right)}{7\overline{M}_1^2 - 1}\left[\frac{A'}{A} \Delta X_s - \frac{\overline{M}_1^2 - 1}{\overline{M}_1\left(1 + 0.2\,\overline{M}_1^2\right)^{1/2}} \frac{\Delta\dot{X}_s}{\overline{a}_T}\right] \tag{65}$$

Equations (65), (60), and (42) relate shock position to perturbations in flow, total pressure, and entropy. Although valid for both upstream and downstream disturbances, consideration is hereinafter restricted to downstream perturbations, and these equations become

$$\frac{\Delta P_{T,2}}{\overline{P}_{T,2}} = -C_1 L_T \frac{A'}{A} \frac{\Delta X_s}{L_T} - C_1 C_2 \frac{d}{dt} \frac{\Delta X_s}{L_T} \tag{66}$$

$$\frac{\Delta \dot{W}_2}{\overline{\dot{W}}} = C_3 \frac{d}{dt} \frac{\Delta X_s}{L_T} \tag{67}$$

$$\frac{\Delta S_2}{R} = C_1 L_T \frac{A'}{A} \frac{\Delta X_s}{L_T} - C_1 C_3 \frac{d}{dt} \frac{\Delta X_s}{L_T} \tag{68}$$

where

$$\left.\begin{aligned} C_1 &= \frac{7\left(\overline{M}_1^2 - 1\right)}{7\overline{M}_1^2 - 1} \\ C_2 &= \frac{5\left(1 + 0.2\ \overline{M}_1^2\right)^{1/2}}{6\overline{a}_T\overline{M}_1} L_T \\ C_3 &= \frac{1}{\overline{a}_T\overline{M}_1} \frac{\overline{M}_1^2 - 1}{\left(1 + 0.2\ \overline{M}_1^2\right)^{1/2}} L_T \end{aligned}\right\} \tag{69}$$

If initial conditions are assumed to be equal to zero, equations (66) to (68) can be written in terms of the Laplace transform as

$$\left.\begin{aligned} \widetilde{P}_2 &= -C_1\left(L_T \frac{A'}{A} + C_2 s\right)\widetilde{X}_s \\ \widetilde{\dot{W}}_2 &= C_3 s \widetilde{X}_s \\ \widetilde{S}_2 &= C_1\left(L_T \frac{A'}{A} - C_3 s\right)\widetilde{X}_s \\ &\text{where} \\ \widetilde{P} &= \frac{\Delta P_T(s)}{\overline{P}_T} \\ \widetilde{\dot{W}} &= \frac{\Delta \dot{W}(s)}{\overline{\dot{W}}} \\ \widetilde{S} &= \frac{\Delta S(s)}{R} \end{aligned}\right\} \tag{70}$$

It should be noted that in equations (42), (60), (65) to (68), and (70) the subscripts or station numbers refer to stations adjacent to and moving with the normal shock. To use the equations in conjunction with other relations describing the subsonic duct, it is desirable to transfer to the primed fixed stations shown in sketch b.

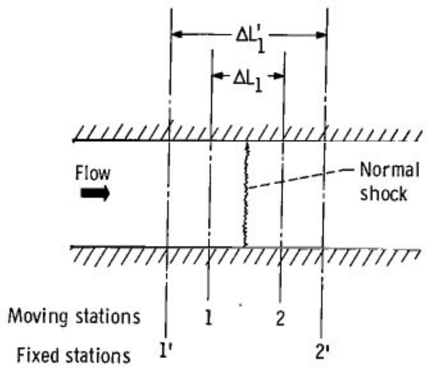

(b)

The distance between primed and unprimed stations need only be greater than the shock motion. In the steady state, total pressure, flow, and entropy are identical at the primed and unprimed stations. Dynamically, they differ only by the time required for a disturbance to propagate between the stations, and for small perturbations the total pressure, flow, and entropy may be regarded as equal at the primed and unprimed stations. The subscripts in equations (42), (60), (65) to (68), and (70) can be referred to either moving or fixed stations.

APPENDIX C

SUBSONIC-DUCT EQUATIONS

The relations for the subsonic portion of the inlet can be derived from the continuity, momentum, and energy equations. The manipulation required to formulate a usable set of equations in terms of the chosen variables (total pressure, flow, and entropy) is outlined in the following section.

For quasi-one-dimensional flow the continuity equation can be written as

$$\frac{\partial}{\partial x}(\rho A v) + \frac{\partial}{\partial t}(\rho A) = 0 \tag{71}$$

or

$$\frac{\partial \dot{W}}{\partial x} + \rho \frac{\partial A}{\partial t} + A \frac{\partial \rho}{\partial t} = 0 \tag{72}$$

From an equation of state of the form

$$\frac{P}{\rho^k} = \frac{P_r}{\rho_r^k} \exp\left(\frac{S - S_r}{C_v}\right) \tag{73}$$

it can be shown that

$$d\rho = \frac{g}{a^2} dP - \frac{\rho}{C_p} dS \tag{74}$$

and the continuity equation becomes

$$\frac{\partial \dot{W}}{\partial x} + \rho \frac{\partial A}{\partial t} + \frac{Ag}{a^2} \frac{\partial P}{\partial t} - \frac{A\rho}{C_p} \frac{\partial S}{\partial t} = 0 \tag{75}$$

The $\Theta\, dS$ equations for both total and static pressures are as follows:

$$\Theta\, dS = C_p\, d\Theta - \frac{dP}{\rho} \tag{76}$$

$$\Theta_T \, dS = C_p \, d\Theta_T - \frac{dP_T}{\rho_T} \tag{77}$$

Subtracting equation (76) from equation (77)

$$(\Theta_T - \Theta)dS = C_p \, d(\Theta_T - \Theta) - \left(\frac{dP_T}{\rho_T} - \frac{dP}{\rho}\right) \tag{78}$$

or, noting that $\Theta_T - \Theta = v^2/2gC_p$, equation (78) becomes

$$dP = \frac{\rho}{\rho_T} \, dP_T - \frac{\rho v}{g} \, dv + \frac{\rho v^2}{2gC_p} \, dS \tag{79}$$

From the relation $\dot{W} = \rho A v$

$$dv = \frac{1}{\rho A} \, d\dot{W} - \frac{v}{\rho} \, d\rho - \frac{v}{A} \, dA \tag{80}$$

Equations (74), (79), and (80) can be combined to yield

$$\left(1 - \frac{v^2}{a^2}\right) dP = \frac{\rho}{\rho_T} \, dP_T - \frac{v}{Ag} \, d\dot{W} + \frac{\rho v^2}{Ag} \, dA - \frac{\rho v^2}{2gC_p} \, dS \tag{81}$$

from which $\partial P/\partial t$ can be determined and substituted into equation (75). The resulting form of the continuity equation is

$$\frac{v}{a^2} \frac{\partial \dot{W}}{\partial t} + \left(\frac{v^2}{a^2} - 1\right) \frac{\partial \dot{W}}{\partial x} - \frac{Ag\rho}{a^2 \rho_T} \frac{\partial P_T}{\partial t} + \frac{A\rho}{C_p} \left(1 - \frac{v^2}{2a^2}\right) \frac{\partial S}{\partial t} - \rho \frac{\partial A}{\partial t} = 0 \tag{82}$$

For quasi-one-dimensional flow of an inviscid fluid the equation of motion is given (see ref. 10) as

$$\rho \frac{\partial v}{\partial t} + \rho v \frac{\partial v}{\partial x} = -g \frac{\partial P}{\partial x} \tag{83}$$

Multiplying equation (83) by A and summing with the continuity equation (71) multiplied by the velocity v give

$$v\frac{\partial}{\partial t}(\rho A) + \rho A\frac{\partial v}{\partial t} + v\frac{\partial}{\partial x}(\rho A v) + \rho A v\frac{\partial v}{\partial x} = -gA\frac{\partial P}{\partial x} \tag{84}$$

Noting that ρAv is the flow $\dot{W}$, equation (84) becomes the momentum equation written in terms of flow.

$$\frac{\partial \dot{W}}{\partial t} + v\frac{\partial \dot{W}}{\partial x} + \dot{W}\frac{\partial v}{\partial x} + gA\frac{\partial P}{\partial x} = 0 \tag{85}$$

Substituting $\partial P/\partial x$, determined from equation (79), into equation (85) yields

$$\frac{\partial \dot{W}}{\partial t} + v\frac{\partial \dot{W}}{\partial x} + \frac{gA\rho}{\rho_T}\frac{\partial P_T}{\partial x} + \frac{\rho A v^2}{2C_p}\frac{\partial S}{\partial x} = 0 \tag{86}$$

Multiplying equation (86) by $(\pm 1 + v/a)$, adding $-a$ times equation (82), and assuming $k = 1.4$ give the following pair of equations:

$$\frac{A\rho g}{a\rho_T}\left[\frac{\partial P_T}{\partial t} + (a + v)\frac{\partial P_T}{\partial x}\right] + \left[\frac{\partial \dot{W}}{\partial t} + (a + v)\frac{\partial \dot{W}}{\partial x}\right]$$

$$= -\frac{A\rho a}{7R}\left[(M^2 - 2)\frac{\partial S}{\partial t} + M^2(a + v)\frac{\partial S}{\partial x}\right] - a\rho\frac{\partial A}{\partial t} \tag{87}$$

$$\frac{A\rho g}{a\rho_T}\left[\frac{\partial P_T}{\partial t} + (v - a)\frac{\partial P_T}{\partial x}\right] - \left[\frac{\partial \dot{W}}{\partial t} + (v - a)\frac{\partial \dot{W}}{\partial x}\right]$$

$$= -\frac{A\rho a}{7R}\left[(M^2 - 2)\frac{\partial S}{\partial t} + M^2(v - a)\frac{\partial S}{\partial x}\right] - a\rho\frac{\partial A}{\partial t} \tag{88}$$

The energy equation for an inviscid non-heat-conducting fluid is given in reference 10 as

$$\Theta\left(\frac{\partial S}{\partial t} + v\frac{\partial S}{\partial x}\right) = \frac{dQ}{dt} \tag{89}$$

or, with no heat addition,

$$\frac{\partial S}{\partial t} + v\,\frac{\partial S}{\partial x} = 0 \qquad (90)$$

Multiplying equation (90) by $2(M + 1)$ and noting that $v = Ma$ gives

$$(2M + 2)\,\frac{\partial S}{\partial t} + 2M(a + v)\,\frac{\partial S}{\partial x} = 0 \qquad (91)$$

Similarly, equation (90) multiplied by $2(1 - M)$ yields

$$(2 - 2M)\,\frac{\partial S}{\partial t} + 2M(a - v)\,\frac{\partial S}{\partial x} = 0 \qquad (92)$$

Adding equations (87) and (91) and equations (88) and (92) results in

$$\frac{g}{a\rho_T}\left[\frac{\partial P_T}{\partial t} + (a + v)\,\frac{\partial P_T}{\partial x}\right] + \frac{1}{A\rho}\left[\frac{\partial \dot{W}}{\partial t} + (a + v)\,\frac{\partial \dot{W}}{\partial x}\right]$$

$$+ \frac{aM(M + 2)}{7R}\left[\frac{\partial S}{\partial t} + (a + v)\,\frac{\partial S}{\partial x}\right] + \frac{a}{A}\,\frac{\partial A}{\partial t} = 0 \qquad (93)$$

and

$$\frac{g}{a\rho_T}\left[\frac{\partial P_T}{\partial t} + (v - a)\,\frac{\partial P_T}{\partial x}\right] - \frac{1}{A\rho}\left[\frac{\partial \dot{W}}{\partial t} + (v - a)\,\frac{\partial \dot{W}}{\partial x}\right]$$

$$+ \frac{aM(M - 2)}{7R}\left[\frac{\partial S}{\partial t} + (v - a)\,\frac{\partial S}{\partial x}\right] + \frac{a}{A}\,\frac{\partial A}{\partial t} = 0 \qquad (94)$$

Equations (93), (94), and (90) can be used to represent the subsonic duct. With a change in notation this set becomes

$$\left.\begin{aligned}
&\frac{g}{a\rho_T}\frac{\delta^+ P_T}{\delta t} + \frac{1}{A\rho}\frac{\delta^+ \dot{W}}{\delta t} + \frac{aM(M+2)}{7R}\frac{\delta^+ S}{\delta t} + \frac{a}{A}\frac{\partial A}{\partial t} = 0 \\
&\frac{g}{a\rho_T}\frac{\delta^- P_T}{\delta t} - \frac{1}{A\rho}\frac{\delta^- \dot{W}}{\delta t} + \frac{aM(2-M)}{7R}\frac{\delta^- S}{\delta t} + \frac{a}{A}\frac{\partial A}{\partial t} = 0 \\
&\frac{\partial S}{\partial t} + v\frac{\partial S}{\partial x} = 0 \\
&\text{where} \\
&\frac{\delta^{\pm}}{\delta t} = \frac{\partial}{\partial t} + (v \pm a)\frac{\partial}{\partial x}
\end{aligned}\right\} \tag{95}$$

When slow area change $\partial A/\partial t \cong 0$ and small perturbations about an equilibrium condition are assumed, equations (95) become

$$\left[\frac{\partial}{\partial t} + (v+a)\frac{\partial}{\partial x}\right]\left[\frac{\Delta P_T}{\overline{P}_T} + \frac{7\overline{M}}{\overline{M}^2+5}\frac{\Delta\dot{W}}{\overline{\dot{W}}} + \frac{\overline{M}(\overline{M}+2)}{\overline{M}^2+5}\frac{\Delta S}{R}\right] = 0 \tag{96}$$

$$\left[\frac{\partial}{\partial t} + (v-a)\frac{\partial}{\partial x}\right]\left[\frac{\Delta P_T}{\overline{P}_T} - \frac{7\overline{M}}{\overline{M}^2+5}\frac{\Delta\dot{W}}{\overline{\dot{W}}} - \frac{\overline{M}(2-\overline{M})}{\overline{M}^2+5}\frac{\Delta S}{R}\right] = 0 \tag{97}$$

$$\left(\frac{\partial}{\partial t} + v\frac{\partial}{\partial x}\right)\frac{\Delta S}{R} = 0 \tag{98}$$

With the substitutions

$$\alpha = \frac{7M_{av}}{M_{av}^2 + 5}$$

$$\beta = \frac{M_{av}(2 + M_{av})}{M_{av}^2 + 5}$$

and

$$\gamma = \frac{M_{av}(2 - M_{av})}{M_{av}^2 + 5}$$

where M_{av} is the steady-state Mach number averaged across the section, equations (96) to (98) become

$$\left.\begin{aligned}
&\left[\frac{\partial}{\partial t} + (v + a)\frac{\partial}{\partial x}\right]\left(\frac{\Delta P_T}{\overline{P}_T} + \alpha\frac{\Delta\dot{W}}{\overline{\dot{W}}} + \beta\frac{\Delta S}{R}\right) = 0 \\
&\left[\frac{\partial}{\partial t} + (v - a)\frac{\partial}{\partial x}\right]\left(\frac{\Delta P_T}{\overline{P}_T} - \alpha\frac{\Delta\dot{W}}{\overline{\dot{W}}} - \gamma\frac{\Delta S}{R}\right) = 0 \\
&\left(\frac{\partial}{\partial t} + v\frac{\partial}{\partial x}\right)\frac{\Delta S}{R} = 0
\end{aligned}\right\} \tag{99}$$

With the further substitution

$$\left.\begin{aligned}
\xi &= \frac{\Delta P_T}{\overline{P}_T} + \alpha\frac{\Delta\dot{W}}{\overline{\dot{W}}} + \beta\frac{\Delta S}{R} \\
\mathscr{E} &= \frac{\Delta P_T}{\overline{P}_T} - \alpha\frac{\Delta\dot{W}}{\overline{\dot{W}}} - \gamma\frac{\Delta S}{R} \\
\eta &= \frac{\Delta S}{R}
\end{aligned}\right\} \tag{100}$$

the set becomes

$$\left.\begin{aligned}
&\left[\frac{\partial}{\partial t} + (v + a)\frac{\partial}{\partial x}\right]\xi = 0 \\
&\left[\frac{\partial}{\partial t} + (v - a)\frac{\partial}{\partial x}\right]\mathscr{E} = 0 \\
&\left(\frac{\partial}{\partial t} + v\frac{\partial}{\partial x}\right)\eta = 0
\end{aligned}\right\} \tag{101}$$

For the typical section of subsonic duct illustrated in sketch c,

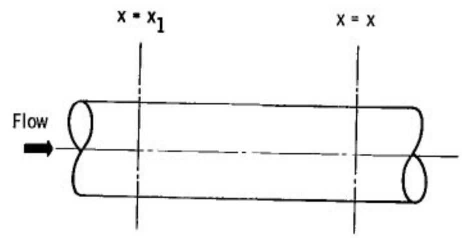

(c)

the general solution of equations (101) is

$$\left.\begin{aligned}
\xi(x, t) &= \xi\left(x_1, t - \frac{x - x_1}{v + a}\right) \\
\mathscr{E}(x, t) &= \mathscr{E}\left(x_1, t - \frac{x - x_1}{v - a}\right) \\
\eta(x, t) &= \eta\left(x_1, t - \frac{x - x_1}{v}\right)
\end{aligned}\right\} \tag{102}$$

This solution represents a pure delay; thus,

$$\left.\begin{aligned}
\xi(x, s) &= \exp\left[-\frac{s}{v + a}(x - x_1)\right]\xi(x_1, s) \\
\mathscr{E}(x, s) &= \exp\left[\frac{s}{a - v}(x - x_1)\right]\mathscr{E}(x_1, s) \\
\eta(x, s) &= \exp\left[-\frac{s}{v}(x - x_1)\right]\eta(x_1, s)
\end{aligned}\right\} \tag{103}$$

If the variable x is set equal to x_2, the length of the segment of duct is $L = x_2 - x_1$, and equations (103) can be written as

$$\left.\begin{aligned} \tilde{P}_2 + \alpha\tilde{\dot{W}}_2 + \beta\tilde{S}_2 &= e^{-\sigma s}\left(\tilde{P}_1 + \alpha\tilde{\dot{W}}_1 + \beta\tilde{S}_1\right) \\ \tilde{P}_2 - \alpha\tilde{\dot{W}}_2 - \gamma\tilde{S}_2 &= e^{\tau s}\left(\tilde{P}_1 - \alpha\tilde{\dot{W}}_1 - \gamma\tilde{S}_1\right) \\ \tilde{S}_2 &= e^{-\theta s}\left(\tilde{S}_1\right) \end{aligned}\right\} \tag{104}$$

where

$$\left.\begin{aligned} \sigma &= \frac{x_2 - x_1}{v + a} = \frac{L}{v + a} \\ \tau &= \frac{x_2 - x_1}{a - v} = \frac{L}{a - v} \\ \theta &= \frac{x_2 - x_1}{v} = \frac{L}{v} \\ \tilde{P} &= \frac{\Delta P_T(s)}{\bar{P}_T} \\ \tilde{\dot{W}} &= \frac{\Delta\dot{W}(s)}{\bar{\dot{W}}} \\ \tilde{S} &= \frac{\Delta S(s)}{R} \end{aligned}\right\} \tag{105}$$

REFERENCES

1. Kantrowitz, Arthur: The Formation and Stability of Normal Shock Waves in Channel Flows. NACA TN 1225, 1947.

2. Sterbentz, William H.; and Evvard, John C.: Criterions for Prediction and Control of Ram-Jet Flow Pulsations. NACA TN 3506, 1955.

3. Himmel, Seymour C.: Application of the Method of Coordinate Perturbation to Unsteady Duct Flows. NACA TM 1439, 1958.

4. Walitt, Leonard: On the Dynamics of a Supercritical Inlet. M. S. Thesis, Univ. California at Los Angeles, 1962.

5. Hurrell, Herbert G.: Analysis of Shock Motion in Ducts During Disturbances in Downstream Pressure. NACA TN 4090, 1957.

6. Wasserbauer, Joseph F.; and Whipple, Daniel L.: Experimental Investigation of the Dynamic Response of a Supersonic Inlet to External and Internal Disturbances. NASA TM X-1648, 1968.

7. Sansom, Frederick J.; and Petersen, Harry E.: Mimic Programming Manual. Rep. SEG-TR-67-31, Aeronautical Systems Div., Wright-Patterson AFB, July 1967. (Available from DDC as AD-656301.)

8. Stitt, Leonard E.; and Salmi, Reino J.: Performance of a Mach 3.0 External-Internal-Compression Axisymmetric Inlet at Mach Numbers from 2.0 to 3.5. NASA TM X-145, 1960.

9. Anon.: Handbook of Analog Computation. Second ed., Electronic Associates, Inc., 1965.

10. Pai, Shih-i: Introduction to the Theory of Compressible Flow. D. Van Nostrand Co., Inc., 1959.

NATIONAL AERONAUTICS AND SPACE ADMINISTRATION
WASHINGTON, D. C. 20546

OFFICIAL BUSINESS

FIRST CLASS MAIL

POSTAGE AND FEES PAID
NATIONAL AERONAUTICS AND
SPACE ADMINISTRATION

010 001 26 51 30S 68351 00903
AIR FORCE WEAPONS LABORATORY/AFWL/
KIRTLAND AIR FORCE BASE, NEW MEXICO 8711

ATT E. LOU BOWMAN, ACTING CHIEF TECH. LI

POSTMASTER: If Undeliverable (Section 158 Postal Manual) Do Not Return

"The aeronautical and space activities of the United States shall be conducted so as to contribute . . . to the expansion of human knowledge of phenomena in the atmosphere and space. The Administration shall provide for the widest practicable and appropriate dissemination of information concerning its activities and the results thereof."

—NATIONAL AERONAUTICS AND SPACE ACT OF 1958

NASA SCIENTIFIC AND TECHNICAL PUBLICATIONS

TECHNICAL REPORTS: Scientific and technical information considered important, complete, and a lasting contribution to existing knowledge.

TECHNICAL NOTES: Information less broad in scope but nevertheless of importance as a contribution to existing knowledge.

TECHNICAL MEMORANDUMS: Information receiving limited distribution because of preliminary data, security classification, or other reasons.

CONTRACTOR REPORTS: Scientific and technical information generated under a NASA contract or grant and considered an important contribution to existing knowledge.

TECHNICAL TRANSLATIONS: Information published in a foreign language considered to merit NASA distribution in English.

SPECIAL PUBLICATIONS: Information derived from or of value to NASA activities. Publications include conference proceedings, monographs, data compilations, handbooks, sourcebooks, and special bibliographies.

TECHNOLOGY UTILIZATION PUBLICATIONS: Information on technology used by NASA that may be of particular interest in commercial and other non-aerospace applications. Publications include Tech Briefs, Technology Utilization Reports and Notes, and Technology Surveys.

Details on the availability of these publications may be obtained from:

SCIENTIFIC AND TECHNICAL INFORMATION DIVISION

NATIONAL AERONAUTICS AND SPACE ADMINISTRATION

Washington, D.C. 20546